J. Biomed. Eng. Res.
Vol.26, No.4, 231-241, 2005

# Co-registration of Multiple Postmortem Brain Slices to Corresponding MRIs Using Voxel Similarity Measures and Slice-to-Volume Transformation

Tae-Seong Kim

Department of Biomedical Engineering, College of Electronics and Information, Kyung Hee University,
*(Received July 19, 2005. Accepted August 4, 2005)*

**Abstract:** New methods to register multiple hemispheric slices of the postmortem brain to anatomically corresponding in-vivo MRI slices within a 3D volumetric MRI are presented. Gel-embedding and fiducial markers are used to reduce geometrical distortions in the postmortem brain volume. The registration algorithm relies on a recursive extraction of warped MRI slices from the reference MRI volume using a modified non-linear polynomial transformation until matching slices are found. Eight different voxel similarity measures are tested to get the best co-registration cost and the results show that combination of two different similarity measures shows the best performance. After validating the implementation and approach through simulation studies, the presented methods are applied to real data. The results demonstrate the feasibility and practicability of the presented co-registration methods, thus providing a means of MR signal analysis and histological examination of tissue lesions via co-registered images of postmortem brain slices and their corresponding MRI sections. With this approach, it is possible to investigate the pathology of a disease through both routinely acquired MRIs and postmortem brain slices, thus improving the understanding of the pathological substrates and their progression.

**Key words:** Co-registration, Postmortem brain slices, MRI, Voxel similarity costs, Slice-to-volume transformation.

## INTRODUCTION

Stereological counting of cells in tissue samples drawn from postmortem brain slices is commonly employed in the study of Alzheimer disease (AD) and subcortical ischemic vascular dementia (SIVD) to analyze cortical and subcortical changes of pathological substrates. However, neither cell counting nor the postmortem brain slices fully reflect changes in pathology. In clinical evaluations, magnetic resonance imaging (MRI) is a powerful tool to detect pathological changes since it provides excellent cortical and subcortical differentiation and serial MRIs show the progression of disease in time. Patients with small-vessel ischemia and AD show white matter lesions (WML), hippocampal and cortical atrophy, and lacunar infarcts [1]. Some of these lesions cannot be identified grossly in the postmortem brain, but MRI can detect significant abnormalities in cortical and subcortical regions.

Thus, relating corresponding MR slices to given postmortem brain slices can provide an objective quantification of pathology through MR signal characterization, leading to improvements in the identification and understanding of a specific disease and its pathological mechanism. This procedure may also yield additional pathological information not obtainable from postmortem slices alone. However, co-registering the postmortem slices to corresponding MR slices within a premortem volume MRI is a challenging task for a number of reasons: 1) the time lapse between the premortem MRI and postmortem brain creates structural discrepancy. This could be prevented by a postmortem MRI [2], but it is known that MR signals decay within the first 90 hours after death carrying no meaningful clinical information [3], 2) the postmortem brain slices are prone to geometrical distortions or multiple deformations due to mechanical slicing, dehydration, and structural collapse. Such distortions were investigated via deformation statistics in [4], and 3) the variability in the thickness and orientation of postmortem brain slices makes dense 3D-volume reconstruction of the postmortem brain

This study was supported by a grant of the Korea Health 21 R&D Project, Ministry of Health and Welfare, Republic of Korea (02-PJ3-PG6-EV07-0002)
**Corresponding Author** : Tae-Seong Kim, Ph.D., Department of Biomedical Engineering College of Electronics and Informations Kyung Hee University 1 Seochun, Kiheung, Yongin, Kyungki, 449-701, Republic of Korea
Tel. +82-31-201-3731
E-mail. tskim@khu.ac.kr

difficult. Therefore, previous attempts to correlate MRI to the postmortem brain have been limited to local structures of interest imaged and sectioned in the corresponding planes, not on a slice-to-slice matching basis [5,6,7].

Although there are various available image registration techniques based on pixel intensity or model matching strategies [8,9,10,11,12,13], application of these existing registration methods to the postmortem-to-MRI co-registration is limited by problems of pixel-voxel size matching, scaling, global and local geometrical distortions, and coarsely reconstructed postmortem brain volume. For instance, the intensity-based approaches [9,10,11,12,13] attempt to match one image volume to the other. However this requires evenly sliced and orientation-preserved slices and relatively comparable voxel characteristics such as PET-PET, MRI-MRI, or PET-MRI. As for the model-based approaches, they generally require geometrical representation of structures based on points, curves, and surfaces. However, identifying these features requires the assistance of experienced anatomists and it is often difficult to identify the exact same features in repeated trials. Moreover, such structural models are not readily available for the postmortem brain associated with different pathological states.

As summarized, co-registration of coarsely sampled pathological sections to postmortem MRIs is one of the most difficult and ill-posed problems in registration since it mainly involves 1) anatomical distortions with unknown mathematical representations and 2) handling quite different inter-modality data. To overcome some of the mentioned difficulties, a very sophisticated method based on cryo-sectioning [8] has been used in an attempt to co-register postmortem slices to MRI. However, the warping mechanism in their physical continuum model, demands heavy computation and is time-consuming, preventing their methodology from general use in studying the correlation of postmortem slices and MRIs.

By taking a rather pragmatic approach, a set of standardized procedures has been developed for handling the postmortem brain via gel-embedding which produces data with minimal geometrical distortions suitable for co-registration [14] and an algorithm to co-register each postmortem brain slice to its corresponding MR sections on a *single whole* slice basis using a 'slice-to-volume' mapping and the mean-squared error (MSE) as a registration cost [15,16]. The feasibility of co-registration was demonstrated by showing that the developed approach provides enough localization for the lesions such as lacunar infarcts, thus allowing further histological examination as demonstrated in [17].

In this study, an improved strategy in accuracy and efficiency to register *multiple hemispheric* postmortem brain slices to their corresponding MR images is presented using a 'multiple slice-to-volume' transformation. The method relies on multiple warped MR images derived recursively from a reference MR volume using modified $n^{th}$-order non-linear polynomials. Furthermore, seven different voxel similarity measures, in addition to the MSE, have been employed and tested, showing that improvements in the registration are achieved by augmenting two similarity measures. After evaluating the registration algorithms with simulation studies where the "ground truth" is known, each similarity measure was applied to real postmortem and MRI data, and evaluated based on difference images and a count of the mismatched pixels [10]. The results demonstrate that the presented approaches including gel-embedding and hemispheric multiple-slice co-registration improve significantly the performance of co-registration. Partial preliminary results in this paper have been presented previously [18].

## MATERIALS AND METHODS

### Preprocessing of Postmortem Brain Images

The preparation of postmortem brain slice images for co-registration is described in [14]. In summary, the specimens of postmortem brains were fixed in 10% neutral formalin for at least two weeks, and sectioned into 28-32 5mm thick coronal slices using a motor-driven rotary slicer. Each slice was then photographed digitally and stored in the Kodak PhotoCD RGB color format at a resolution of 3072x2048, keeping an in-plane spatial resolution of approximately 0.5mm. The brain was extracted from the background of the RGB postmortem photographs by selectively thresholding RGB intensity values, and converted to gray-scale by eliminating the hue and saturation while retaining the luminance information. In handling the postmortem brain, maintaining a relative distance between two hemispheres is difficult, since only the corpus callosum connects the hemispheres. Thus, the brain is separated into hemispheres by slicing through the corpus callosum and registered each hemisphere separately. One of the key requirements to register accurately a postmortem brain slice to its corresponding MR slice is to minimize local and global geometrical distortions [16]. To minimize distortions due to mechanical slicing and dehydration, and to reduce the variability in the planar thickness and orientation of the postmortem slices, each hemisphere was embedded in 3% agar gel and a set of coronal brain slices was obtained as shown in Fig. 1 (a). Registration markers, shown as black holes in Fig. 1 (a), were also embedded in the gel and used as control points to realign the slices to form a 3D volume. Figure 1 (b) shows a set of multiple slices after segmenting the brain regions from the background and registering all slices based on the embedded markers via a control point based registration [19]. More details of

standardized procedures for gel-embedding and handling the postmortem brain can be found in [14].

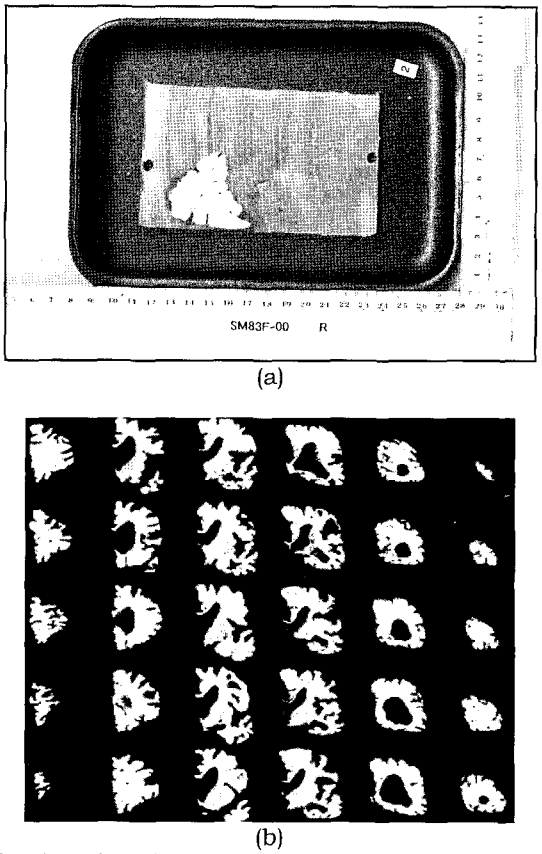


(a)

(b)

**Fig. 1.** (a) A slice of the postmortem brain (right hemisphere) embedded in agar gel. Registration markers are shown as black holes. (b) A set of multiple slices after brain segmentation and control point-based realignment.

## Preprocessing of Pre-mortem MRI

*MRI*

For reference MR images, three types of MRI scans were acquired for eight subjects on a GE 1.5T Signa System: coronal $T_1$-weighted, transaxial Proton Density (PD), and transaxial $T_2$-weighted MRIs respectively. The $T_1$-weighted 3D coronal scan was made using a gradient-echo (SPGR) sequence with TR=24ms, TE=5ms, flip angle=45□, field of view=24x24cm$^2$, 124 slices, slice thickness=1.5mm, and 0.86x0.86 mm$^2$ in-plane resolution. The PD and $T_2$-weighted images were acquired using a dual-echo turbo spin echo (TSE) sequence with TR=45ms, $TE_1$=14ms, $TE_2$=85ms, 51 slices, slice thickness=3mm, and 1.0x1.0mm$^2$ in plane resolution. Due to its higher resolution, coronal $T_1$-weighted MR images were used to form the 3D reference volume.

*MR Brain Extraction and Splitting*

The Brain Surface Extraction (BSE) algorithm [20], which extracts the brain regions using a morphological process, was used to strip off the skull and scalp in MR images. In addition, the regions of pons and cerebellum were removed manually from each MR slice, since these regions were absent in the postmortem slices. To match the slices of each hemisphere of the postmortem brain, each extracted MR brain volume was also cut into two hemispheres through the inter-hemispheric fissure and stored separately.

## Multiple Slice Slice-to-Volume Transformation

In addition to geometrical distortions, a complicating factor in co-registration is that, unlike MRI, the photographed side of the postmortem slices does not reflect voxel information but only surface optical reflectance variations. Thus direct volume-to-volume registration between the two modalities is difficult. To accomplish co-registration within these constraints, a slice-to-volume coordinate transformation for each pixel has been devised incorporating image warping in the coordinate transformation using modified general n$^{th}$-order polynomials in the following manner [15,16,21]:

$$\begin{aligned} u &= a_0 + a_1 i + a_2 j + a_3 i^2 + a_4 ij + a_5 j^2 + \ldots \\ v &= b_0 + b_1 i + b_2 j + b_3 i^2 + b_4 ij + b_5 j^2 + \ldots \\ w &= c_0 + c_1 i + c_2 j + c_3 i^2 + c_4 ij + c_5 j^2 + \ldots \end{aligned} \quad (1)$$

where $(u, v, w)$ is a new coordinate of a voxel in a 3D MRI , $(i, j)$ is a pixel coordinate within a postmortem image, and $a_i$ , $b_i$ , and $c_i$ are image coordinate transformation coefficients.
This can be expressed in a matrix form:

$$y = Kx \quad (2)$$

where $y = [u, v, w]^T$ ,

$$K = \begin{bmatrix} a_0 & a_1 & a_2 & a_3 & a_4 & a_5 & \ldots \\ b_0 & b_1 & b_2 & b_3 & b_4 & b_5 & \ldots \\ c_0 & c_1 & c_2 & c_3 & c_4 & c_5 & \ldots \end{bmatrix},$$

$x = [1 \quad i \quad j \quad i^2 \quad ij \quad j^2 \quad \ldots]^T$ , and $T$ denotes a vector transpose.

Given transformation coefficients $K$ , with an assumption that each slice is separated with a uniform inter-slice distance $d$ , multiple slices can be extracted from a 3D reference image volume $V$ in the following way:

$$M_k = g(f(Y, d), V) = g(f(K, X, d), V) \quad (3)$$

where $M$ represents MR slices with $k = \{1,...,N\}$ and $N$ being the total number of slices, a function $f(\bullet)$ the slice-to-volume transformation, $g(\bullet)$ 3D interpolation, $X$ a set of pixel coordinates, and $Y$ a set of voxel coordinates.

The uniform inter-slice distance assumption is valid only if mechanical slicing produces each slice with a finite thickness and generates the same global distortions. In this study, it is assumed that these criteria are satisfied with the gel-embedding and mechanical slicing.

## Characteristics of Voxel Similarity Measures

A standard approach to estimate the transformation coefficients including the inter-slice distance is to minimize the sum of differences between the given postmortem images and the iteratively extracted and warped MR images, i.e.,

$$(a_i^*, b_i^*, c_i^*, d^*) = \arg\min_{a_i, b_i, c_i, d} \sum_{k=1}^{N} e(P_k, M_k) \qquad (4)$$

where $e$ is a function defining a registration cost, $P$ a set of postmortem images, and $M$ a set of extracted MRI slices.

To measure a degree of matching or registration error between postmortem and MR slices, eight different similarity functions were tested as possible cost functions. These most commonly used similarity functions are based on image intensities, information measures, and object patterns and have been studied by Holdon et al. [22]. Here the characteristics of each measure are briefly reviewed. Their mathematical definitions are available in [22] and [23].

### *Mean-Squared Difference (MSD)*

It is shown that this similarity measure is optimal when image intensity transformation for two images is identical with Gaussian noise [24]. This measure gets minimized to find a matching slice. In the previous study, MSD is extensively tested for a single slice registration [16]. The results demonstrated the feasibility of the approach and produced reasonable co-registration with limited success.

### *Pearson Cross Correlation (PCC)*

If the intensity transformation for pixels is linear, the PCC similarity measure is suggested to be optimal [24]. PCC has been used extensively in co-registering serial MRIs by Lemieux et al. [25].

### *Mutual Information (MI)*

Mutual information measures statistical dependence between two given images; thus by maximizing the common amount of information in the two images we can achieve co-registration. In general, this measure does not require any assumption or preprocessing on the pixel intensity of images. It is also considered to be the optimal choice for multimodal image registration. This measure has been utilized with a rigid body model in the following studies: Maes et al. used MI for co-registering MR-MR, MR-CT, and MR-PET images [26]. Holden at al. used it for co-registering serial MRIs [22], and Kim et al. for co-registering functional MRI-MRI [27]. With a non-rigid model, MI has been also used in the study by Kim et al. where an autoradiograph slice was registered to a reference image on a slice-by-slice basis [28], and Kjems et al. used MI to register volume MRI-PET [11] employing a deformation field model.

### *Normalized Mutual Information (NMI)*

This similarity measure was suggested by Studholme [29] and used to register MR images with a non-rigid model [12] and to register fMRI echo planer images (EPIs) to anatomical MRIs with a geometric distortion model [13].

### *Entropy of Difference Image (EDI)*

This similarity measure was used to remove motion between images in digital subtraction angiography [30]. Co-registration is achieved by minimizing the entropy of difference images.

### *Ratio Image Uniformity (RIU) and Modified RIU (MRIU)*

This similarity measure was proposed by Woods et al. [9] and its modified version was suggested by Holden et al. [22]. RIU has been extensively used in AIR [9] to register MRI-MRI and MRI-PET in 3D. This measure was also extensively utilized for fMR EPI image registration for correcting movement related effects using higher order polynomials [31]. Minimization of his measure achieves co-registration.

### *Modified Pattern Intensity (MPI)*

This similarity measure achieves registration by maximizing the local correlation between selected regions of the images. Weese et al. used this measure to register fluoroscopy images to 3D CT images [32].

*Augmented Cost Functions*

Although each similarity measure demonstrate its own reasoning, in general it is difficult to assess which is the best registration cost. Difficulties in choosing the best registration cost were also studied in the work of Freire et al. [33]. In this study, based on experiences on testing eight similarity measures mentioned above, a two-step registration approach is devised where geometrical distortions are corrected in the first step by co-registering images with MSD or PCC (thus matching the size and shape of the brain first), and then, using the pre-estimated transformation parameters, MI or NMI are used to improve the registration further by matching internal structures and intensity distribution: therefore, if PCC is augmented with MI or NMI, AMI denotes PCC+MI or ANMI denotes PCC+NMI.

### Registration Algorithms

The multiple slice-to-volume transformation translates the coordinates of pixels in the 2D postmortem slices to voxels in the 3D MRI volume. Beginning with initial locations within the MRI volume that produce the minimum difference according to a given cost function, warped 2D sections lying within the 3D MRI volume are derived at every iteration until best-matching MR sections to given postmortem slices are found by optimizing the registration cost. Transformation parameters are estimated using a quasi-Newton-based multidimensional optimization algorithm with a tri-linear or cubic 3D interpolation method [34] producing images at the transformed pixel coordinates. Details of the convergence of the algorithm to different initial conditions and the performance of different polynomial order are given in the previous report [16].

### Validation of Registration Algorithms

In order to validate the implementation and numerical accuracy of the algorithm, computer simulation studies were carried out using only a reference MRI volume. With pre-selected 'true' 2nd-order polynomial transformation coefficients, a set of test MR slices was obtained from the 3D reference MRI volume. Then using this set as the original, co-registration was performed with each similarity measure, resulting in estimated transformation coefficients. The numerical accuracy of each similarity measure was assessed in terms of the Euclidian distance between pixel offsets resulting from the discrepancy between the known and estimated coefficients.

However, in the case of postmortem slice co-Registration, the performance of each measure depends on the nature of the data and it is not possible to model all distortion factors in the postmortem slices. Hence numerical validation is difficult since a "gold standard" cannot be obtained. To evaluate the reliability and accuracy of co-registration with real data, difference images are examined by adopting an index of *voxel mismatch count (VMC) [10] within brain* overlapped regions, where the number of mismatched pixels is determined by counting pixels whose intensity in the difference image >20% of the mean intensity as defined in [10]. In addition to VMC, visual identification of common anatomical landmarks (e.g., anterior commissure, pillars of fornix, perivascular spaces, and optic chiasm) by experienced anatomists was used to verify co-registration.

## RESULTS

### Validation of Algorithms: Simulation Study

The discrepancy of voxel locations due to the estimated transformation coefficients was computed. The mean and standard deviation (SD) of voxel displacements after co-registration using the eight similarity measures were: MSD=0.0183 (SD=0.0085), MI=0.0295 (SD=0.0143), NMI=0.0261 (SD=0.0099), PCC=0.0109 (SD=0.0064), EDI=0.2137 (SD=0.1216), MPI=0.0069 (SD=0.0037), RIU=1.0082 (SD=0.5606), and MRIU=36.2281 (SD=8.2171). Except for RIU and MRIU, the mean voxel displacement error was in the subvoxel range.

### Sensitivity of Cost Functions

Of the eight subjects entered in this study, two cases were dropped due to severe distortions in the outer boundaries of the postmortem slices and in the internal structures including ventricles and one due to severe artifacts in MRI. For the remaining five cases, all eight similarity functions and two augmented cost functions were investigated, and 5-11 hemispheric postmortem slices were co-registered to their corresponding MR slices in a multiple-slice mode using 2nd-order polynomials. Figures 2 (b)-(i) show a typical set of MR slices registered to the postmortem slice shown in Fig. 2 (a) with different registration cost functions. A visual inspection of registered images and difference images indicates that best co-registration was obtained with MSD, PCC, and the augmented cost measures. Overall strong mismatches were noted with MPI, RIU, and MRIU. The prominent anatomical landmarks, including the thalamus, hippocampus, and sub-cortical grey nuclei, appeared to be well registered in the postmortem and MR images.

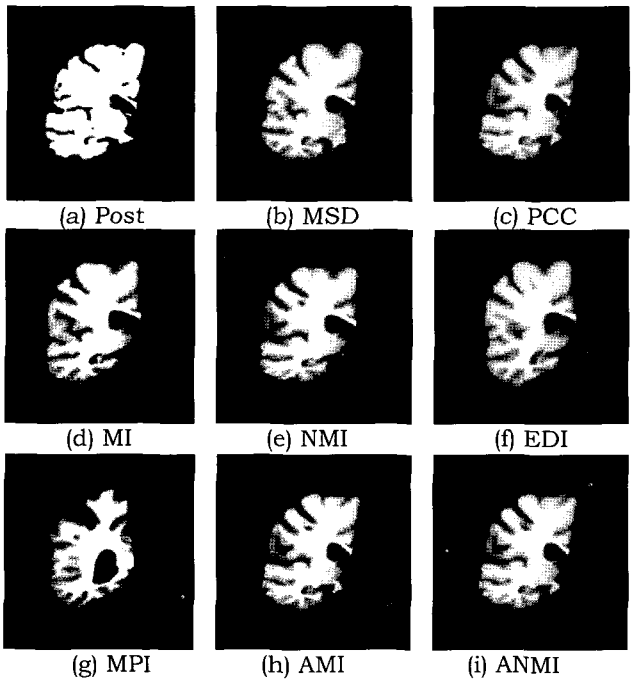


**Fig. 2.** Registration results using various similarity measures. (a) Original postmortem image (b-i) Registered MR slices obtained through different cost measures.

The voxel mismatch counts expressed in percent changes for all five cases and eight similarity measures are summarized in Table 1. Voxel mismatch counts in all cases were normalized by the total number of voxels of the brain and expressed in percent changes to make statistical comparisons across slices and subjects. Although the overall trend in Table 1 suggests that PCC seems to be the best cost, there was an exception for case C1. It was found that when there is less distortion in the postmortem brain slices such as in C1, similarity measures based on probability density such as MI, NMI, and EDI performed better than any other measures. With more distortion in postmortem slices, similarity measures depending on voxel intensity such as MSD and PCC were found to be more sensitive in matching the location, overall shape, and size of the postmortem brain slices, suggesting that these measures are more sensitive for correcting geometrical distortions.

As for the augmented similarity, the voxel mismatch counts expressed in percents in Table 2 for all five cases show a significant reduction compared to the counts in Table 1 indicating that better match was found with the augmented cost. Difference images using the augmented measure showed more uniform gray patches than the difference images of registered images using either similarity measure alone.

The bar plot in Fig. 3 shows the mean and standard deviation of all cases for all similarity measures including the augmented. Although marginal reduction in the counts was obtained with the augmented cost compared to PCC or MSD alone, significant reduction was obtained compared to those of MI or NMI. To obtain a measure of the statistical significance of reduction in the counts for the augmented costs (i.e., AMI and ANMI), the paired t-test was performed with one-tail at the 95% confidence level against other costs [35]. The registration results using AMI were found to be better significantly than those of MSD, MI, and NMI (P=0.0086, 0.0027, and 0.0035) as were the results using ANMI (P=0.0068, 0.0021, and 0.0027). However, when the results using AMI and ANMI were compared with the results using PCC, the improvement was not statistically significant (P=0.0825 and 0.0697).

The augmented approach increased the total computation time by only about 10-15% over that for MSD or PCC alone. Although not verified in this study, it has been observed that MI alone requires more iterations than MSD by a factor of two as shown in [11]. Thus using augmented measures, faster convergence can be obtained with MSD or PCC, and then fine adjustment can be done much faster with MI.

**Table 2.** Normalized Voxel Mismatch Counts for Augmented Registration Costs

| | Mean (Standard Deviation) | |
|---|---|---|
| Case | AMI | ANMI |
| C 1 | 20.36(0.94) | 19.97(1.37) |
| C 2 | 18.25(4.18) | 18.08(4.56) |
| C 3 | 13.96(0.04) | 13.69(0.18) |
| C 4 | 16.05(0.69) | 15.86(0.55) |
| C 5 | 3.28(0.49) | 3.34(0.41) |
| Total | 14.45(6.89) | 14.24(6.77) |

**Table 1.** Normalized Voxel Mismatch Counts for Eight Different Registration Costs

| | Mean (Standard Deviation) of (VMC/Total No. Brain Voxels)*100 | | | | | | | |
|---|---|---|---|---|---|---|---|---|
| Case | MSD | PCC | MI | NMI | EDI | MPI | RIU | MRIU |
| C 1 | 21.99(1.87) | 20.57(0.73) | 20.15(1.70) | 19.96(1.70) | 19.96(1.71) | 39.09(40.61) | 78.81(42.37) | 60.81(45.27) |
| C 2 | 17.81(4.43) | 17.82(4.73) | 22.73(2.87) | 23.35(6.11) | 27.65(2.78) | 56.97(60.85) | 56.89(60.86) | 56.85(60.97) |
| C 3 | 30.17(2.40) | 30.73(1.74) | 31.07(1.18) | 31.78(1.79) | 35.01(1.57) | N/A* | N/A* | N/A* |
| C 4 | 17.67(0.57) | 15.79(1.01) | 18.85(4.88) | 18.93(2.90) | 22.65(0.39) | 16.49(4.14) | 59.75(56.92) | 56.68(61.26) |
| C 5 | 8.646(3.05) | 3.53(0.52) | 19.23(3.19) | 18.35(7.26) | 22.86(1.53) | 44.63(48.33) | 71.89(48.70) | N/A* |
| Total | 18.86(7.46) | 17.04(9.15) | 21.82(4.80) | 21.79(6.00) | 24.54(5.49) | 49.01(42.07) | 74.17(40.34) | 74.64(33.67) |

*No covergence was obtained.

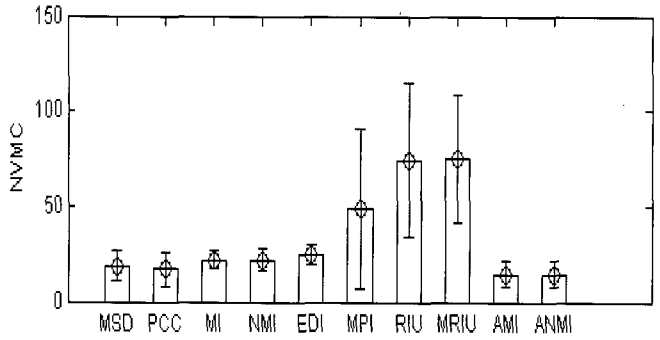


**Fig. 3.** Plot of normalized voxel mismatch count showing mean and standard deviation of each similarity cost.

## Augmented Cost Functions

To simultaneously co-register multiple hemispheric postmotem brain slices to their matching MR images, a stack of images was prepared as discussed in Fig. 1 and all slices within the stack were registered with the augmented cost measure AMI. Two sets of registered images from two different subjects are shown in Figs. 4 and 5.

(a) Consecutive Postmortem Brain Slices

(b) Registered MR Slices using Augmented Cost

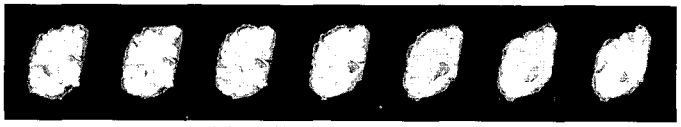

(c) Difference Images

**Fig. 4.** A set of multiple slice registration results. (a) Seven consecutive postmortem slices used to register simultaneously. (b) Registered MR slices show good matching in the size, shape, and internal structures. (c) Gray-scale in the difference images reveals well-matched and mis-matched regions.

The first row of Fig. 4 shows seven postmortem slices of one hemisphere of the postmortem brain, the second row seven co-registered MR images, and the last row the difference images. As indicated in the gray-scale, positive differences are shown brighter and negative differences darker than the mean gray level which indicates zero difference, i.e., a good match.

In Fig. 5, four registered slices out of 10 per hemisphere are shown. The upper rows of Fig. 5 (a) and (b) show the postmortem images and the lower their corresponding registered MRIs. As the registered images demonstrate, there are strong matches in the size, shape, and internal structures of the brain. The anatomical features are well registered in their outer and inner contours include the ventricles, subcortical grey nuclei, hippocampus, corpus callosum, and the choroid plexus within the third ventricle. The mean value of VMC for all slices was 7.57% (min=4.8% and max=16.77%).

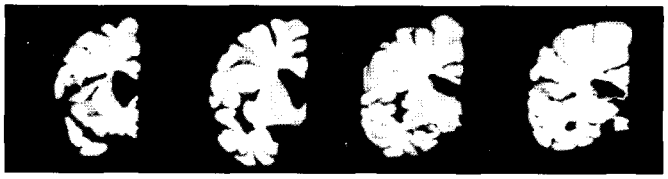

Postmortem images of left hemisphere

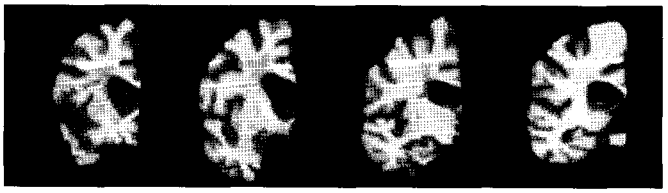

Registered MRIs
(a)

Postmortem images of right hemisphere

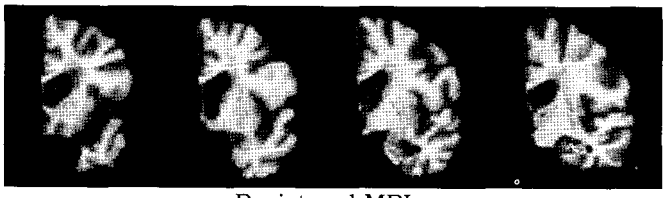

Registered MRIs
(b)

**Fig. 5.** Another set of multiple slice registration results. (a) The upper row shows four postmortem images of the left hemisphere of the brain and the lower registered MRIs. (b) The upper row shows four postmortem images of the right hemisphere and the lower registered MRIs.

### Single-slice vs. Multiple-slice Registration

For the comparison of the co-registration results via a single-slice mode vs. a multiple-slice mode, eleven consecutive postmortem brain slices were registered with two different modes using AMI and 2nd order polynomials. Three representative slices are shown in Fig. 6. From the counts of VMC and visual inspection, it is found that the multiple-slice mode performed better overall. For example, the 3rd column of Fig. 6 shows where the single-slice mode failed, but the multiple-slice mode found all correct slices. However, it is also noticed that when a matching slice was correctly found with the single-slice mode as shown in the second column of Fig. 6, it outperformed the multiple-slice with a lower VMC count. The counts were 5.76, 3.71, and 22.95% for Fig. 6 (b) left-to-right respectively, and 5.11, 6.53, and 5.85% for Fig. 6 (c).

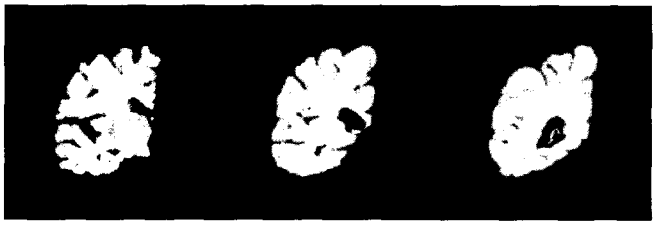

(a) Three slices of postmortem brain

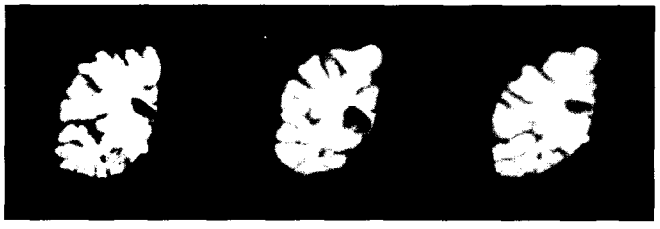

(b) Three registered MRIs using AMI via a single-slice mode

(c) Three registered MRIs using AMI via a multiple-slice mode

**Fig. 6.** Results of co-registering postmortem slices via single-slice and multiple-slice mode. (a) Three postmortem slices. (b) Registered MR slices via a single-slice mode. (c) Three registered MR slices via a multiple-slice mode.

### Postmortem Slices to Longitudinal MRIs

To check the reliability of the registration approach in longitudinal studies, it was also attempted to register postmortem slices to their corresponding MR slices in three longitudinal MR scans performed four years apart. Co-registration was done with a multiple-slice mode, 2nd-order transformation, and AMI as the cost function. The results are presented in Fig. 7. The first row shows four postmortem slices out of twelve, and subsequent rows show their registered MRIs in the longitudinal scans. Visual inspection shows close matches of anatomical structures and the mean VMC values for each longitudinal scan was 9.91%, 10.17%, and 13.85% respectively.

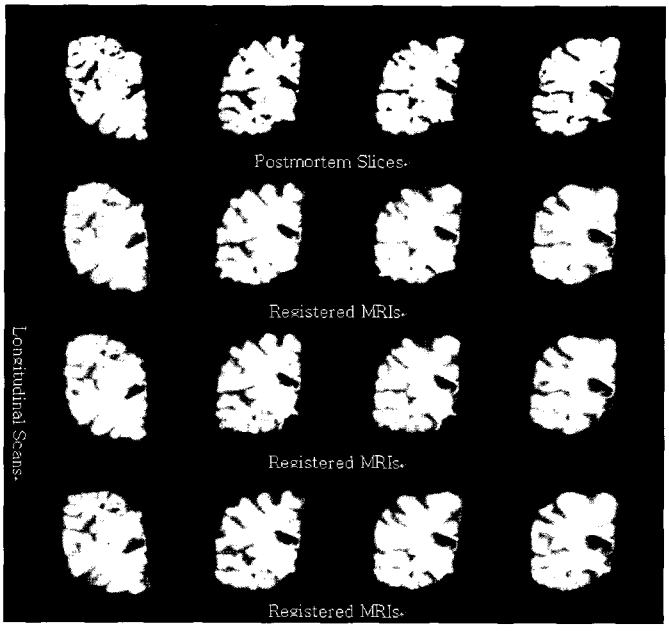


**Fig. 7.** Co-registration results of postmortem slices to three longitudinal MRIs. Four consecutive postmortem slices are shown in the first row. The following each row shows the registered MR images in three longitudinal MR scans.

### Lesion Mapping in the Registered Pair of Postmortem and MRI Slices

One of the main goals of developing the co-registration methodology is to map lesions either found in postmortem slices or MRIs to their corresponding images. In order to demonstrate that the presented methodology provides enough accuracy of lesion mapping for further investigation, first, a lesion is identified in MRI and mapped into the postmortem slice as shown in Fig. 8. This capability allows the localization of ROIs for histological tissue examination

or MR signal analysis of tissues as demonstrated in the separate studies [14,17].

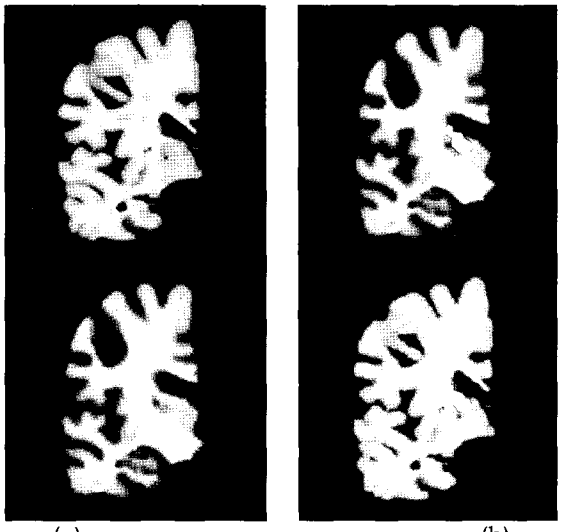


**Fig. 8.** An example of lesion mapping. (a) A pair of postmortem slices (top) and registered MRIs (bottom). (b) Lesion identified in the registered MRI (top) is mapped into the postmortem slice (bottom).

## DISCUSSION

Although pathological information at the cellular level can be derived from postmortem brain tissues, the natural progression of disease can be monitored more efficiently through longitudinal MR scans. The progression of a disease can then be compared to the pathology of brain tissue by co-registering postmortem slices to their corresponding MR slices. The purpose of this work is to provide a methodology for such co-registration between given postmortem slices and MRIs. In fact, knowledge of MR signal changes of pathological substrates may add significant information about the disease to the histological analysis of tissue itself.

The significance of the presented approach lies in its practicability, cost-effectiveness, and minimal expert human intervention. The postmortem brain preparation in gel can be done easily without sophisticated apparatus. There is no need for high-resolution postmortem image volume and no landmark localization or structural model generation is required. Once postmortem and MR images are pre-processed no human intervention is needed to find the matching slices. In general ROIs only reside in a few postmortem slices. Thus only the desired slices need to be registered using a multiple-slice mode. The single-slice mode allows an option of co-registration when accurate realignment into a stack is not possible.

A similar approach to the presented method was independently reported by Kim et al. [27]. In their work, individual slices were registered to an anatomical volume via the "map-slice-to-volume" approach and the use of mutual information to correct motion in fMRI with a rigid body model. However, the presented method is different in its use of nonlinear global correction afforded by the nonlinear polynomial transformation and inter-slice gap handling. Also the sensitivity of various voxel similarity measures were studied and it is found that correlation similarity is more sensitive than mutual information and that the combinatory use of similarity measures is better than a single measure.

It is generally understood that mutual information is the optimal choice for registering multi-modal medical images, especially when images reflect different contrasts. However the results in this study suggest that the correlation measure could be the optimal choice to register postmortem photographs to MRI. This observation could be explained by: (a) Intensity transformation between postmortem photographs and MRI has a linear relationship, thus producing better results as suggested by Viola [24]. More studies are underway to study a larger group of cases for a firmer conclusion, and (b) it is shown that the cost curve for the global maximum for mutual information is much narrower than that of any other cost, and convergence for global maximum heavily depends on the image interpolation and optimization methods [26]. This may explain the reduced performance of MI in this study. The use of simulated annealing optimization procedure [34] is being currently investigated to overcome the limitations of interpolation and optimization.

In this study, mainly the 2nd-order polynomial transformation was tested allowing the following transformations in 3D: translation, rotation, scaling, skewness, and perspective [36]. Although the previous investigation using the 3rd-order [21] showed a significant improvement in registration, it is not clear that further expansion of polynomial order would produce better co-registration. However, as demonstrated in this study, gel-embedding significantly reduces local distortions and the 2nd-order compensation in the multiple slice mode does seem to be enough to obtain reasonable co-registration. In the case of MRI-MRI registration where structural deformation is not significant, Woods et al. showed marginal improvement of registration with higher number of coefficients [9]. Since higher order of polynomials complicates parameter estimation and demands more computation time, the relation of model order versus registration performance must be investigated.

Although VMC is adapted as an indicator of image matching, it should be acknowledged that it might not reflect correct degree of co-registration and has limitations, since VMC is not a bias-free arbiter of each co-registration cost. Due to the nature of problem, neither voxel or pixel intensity difference measures nor

visual inspection alone reflects the degree of correct co-registration. However, it is believed that the validation approaches should reflect some degree of quantitative and qualitative measures of co-registration. A search for quantitatively accurate measures of co-registration is underway.

Although the merit of non-linear polynomial transformation is its ability to perform spatial transformation with a specified order, the transformation is global and local refining registration mechanism might be more critical to improve the registration accuracy of local regions. To improve local registration at reasonable cost, the possibility of utilizing a local window surrounding a specific anatomical region as attempted in [37] using local Gaussian windows should be investigated.

## CONCLUSION

In this work, a much improved method is presented relying on a slice-to-volume transformation using $n^{th}$-order polynomials to co-register multiple postmortem brain slices to their corresponding MR slices within a reference MR volume. The characteristics of eight different similarity measures were tested to achieve co-registration. The results demonstrate that the combined use of PCC and MI produces better results than any one of the measures alone. The results were supported by visual anatomical comparisons, difference between the postmortem and registered MR images, and the counts of mismatched voxels. With this approach, MR characteristics of a disease can be correlated to the pathology of the disease, thus increasing the clinical significance of MR scans. The co-registration approach used in this study is efficient and provides enough accuracy for histological examination. Also the technique is cost-effective since only those postmortem slices containing the region of interest can be registered, and can be applied automatically with minimum human intervention (i.e., no anatomical templates or structure representations are required).

## REFERENCES


[1] H. M. Wisniewski and J. Wegiel, "*Neuropathology of Alzheimer's disease*", Neuroimaging Clin. N. Am., Vol. 5, pp. 45-57, 1995.

[2] S. Grafton, M. Sumi, G. K Stimac, E. C. Alvord, C. M. Shaw, and D. Nochlin, "*Comparison of postmortem magnetic resonance imaging and neuropathologic findings in the cerebral white matter*", Arch. Neurol., Vol. 48, pp. 293-298, 1991.

[3] G. W. E. Englund, E. M. Larsson, A. Brun, S. Cronqvist, and B. Persson, "*Proton magnetic resonance relaxation times $T_1$ and $T_2$ related to postmortem interval: An investigation on porcine brain tissue*", Acta. Radiol. Diagnosis, Vol. 27, pp. 115, 1986.

[4] T. Schormann, A. Dabringhaus, and K. Zilles, "*Statistics of Deformations in Histology and Application to Improve Alignment with MRI*", IEEE Trans. Med. Imag., Vol. 14, No. 1, pp. 25-35, 1995.

[5] M. R. Grafe, G. A. Press, D. P. Berthoty, J. R. Hesselink, and C. A. Wiley, "*Abnormalities of the brain in AIDS patients: Correlation of postmortem MRI findings with neuropathology*", A. J. N. R., Vol. 11, pp. 905-911, 1990.

[6] P. L. McGeer, H. Kamo, R. Harrop, E. G. McGeer, W. R. W. Martin, B. D. Pate, and D. K. B. Li, "*Comparision of PET, MRI, and CT with pathology in a proven case of Alzheimer's disease*", Neurology, Vol. 36, pp. 1569-1574, 1986.

[7] J. R. Nixon, G. M. Miller, H. Okazaki, and M. R. Gomez, "*Cerebral tuberous sclerosis: Postmortem magnetic resonance imaging and pathologic anatomy*", Mayo Clin. Proc., Vol. 64, pp. 305-311, 1989.

[8] A. W. Toga, An Introduction to Brain Warping. In Brain Warping. Academic Press, San Diego, 1-26, 1999.

[9] R. P. Woods, S. T. Grafton, C. J. Holmes, S. R. Cheery, and J. C. Mazziotta, "*Automated Image Registration: I. General Methods and Intrasubject, Intramodality Validation*", J. Comp. Assisted Tomogr., Vol. 22, No. 1, pp. 139-152, 1998.

[10] P. A. Freeborough, R. P. Woods RP, and N. C. Fox, "Accurate Registration of Serial 3D MR Brain Images and Its Application to Visualizing Change in Neurodegenerative Disorders", J. Comp. Assisted Tomogr., Vol. 20, No. 6, pp. 1012-1022, 1996.

[11] U. Kjems, S. C. Strother, J. Anderson, I. Law, and L. K. Hansen, "*Enhancing the Multivariate Signal of [$^{15}$O] Water PET Studies with a New Nonlinear Neuroanatomical Registration Algorithm*", IEEE Trans. Med. Imag., Vol. 8, No. 4, pp. 306-319, 1999.

[12] C. Studholme, E. Novotny, R. Stokking, J. S. Duncan, I. G. Zubal, and D. Spencer D, "Alignment of Functional Data Acquired Before and After Intra-Cranial Electrode Implantation Using Non-Rigid Anatomical MRI Registration", Proc. Intl. Soc. Mag. Reson. Med., Vol.8, pp.585, 2000.

[13] C. Studholme, R. T. Constable, and J. S. Duncan, "*Accurate Alignment of Functional EPI Data to Anatomical MRI Using a Physics-Based Distortion Model*", IEEE Trans. Med. Imag., Vol. 19, No. 11, pp. 1115-1127, 2000.

[14] C. Zarow, T.-S. Kim, M. Singh, and H. Chui, "*A Standarized Method for Brain Cutting Suitable for Both Stereology and MRI-Brain Coregistration*", J. Neurosci. Methods, Vol. 139, No. 2, pp. 209-215, 2004.

[15] T.-S. Kim, M. Singh, W. Sungkarat, C. Zarow, and H. Chui, "*Registration of In-Vivo MRI to Postmortem Brain Photographs*", Proc. Intl. Soc. Mag. Res. Med., Vol.8, pp.677, 2000.

[16] T.-S. Kim, M. Singh, W. Sungkarat, C. Zarow, and H. Chui, "*Automatic Registration of Postmortem Brain Slices to MRI Reference Volume*", IEEE Trans. Nucl. Sci., Vol. 47, No. 4, pp. 1607-1613, 2000.

[17] T.-S. Kim, M. Singh, S. Kim, C. Zarow, W. G. Ellis, and H. Chui, "*MRI-Guided Histological Analysis of Postmortem Brain Slices*", Proc. Intl. Soc. Mag. Res. Med., Vol.11, pp.2255, 2003.

[18] T.-S. Kim, M. Singh, S. Kim, C. Zarow, and H. Chui, "*Simultaneous Registration of Multiple Postmortem Bran Slice Images to their Corresponding MRIs*", Proc. Intl. Soc. Mag. Res. Med., Vol.10, 2002.

[19] M. Singh, W. Frei, and T. Shibata, "A digital technique for accurate change detection in nuclear medicine images with applications to myocardial perfusion studies using

thallium-201", IEEE Trans. Nucl. Sci., Vol. 26, pp. 565-575, 1979.

[20] S. Sandor and R. Leahy, "*Surface-Based Labeling of Cortical Anatomy Using a Deformable Atlas*", IEEE Trans. Med. Imag., Vol. 16, No. 1, pp. 41-54, 1997.

[21] T.-S. Kim, M. Singh, N. Ghugre, S. Kim, C. Zarow, and H. Chui, "*Registration of Postmortem Brain Slices to Matching MR Slices within 3D Reference MRI*", Proc. Intl. Soc. Mag. Res. Med., 814, 2001.

[22] M. Holden, D. L. G. Hill, E. R. E. Denton, J. M. Jarosz, T. C. S. Cox, T. Rohlfing, J. Goodey, and D. J. Hawkes, "*Pixel Similarity Measures for 3-D Serial MR Brain Image Registration*", IEEE Trans. Med. Imag., Vol. 19, No. 2, pp. 94-102, 2000.

[23] J. V. Hajnal, N. Saeed, E. J. Soar, A. Oatridge, I. R. Young, and G. M. Bydder, "*A registration and interpolation procedure for subpixel matching of serially acquired MR images*", J. Comp. Assisted Tomogr., Vol. 19, No. 289-296, 1995.

[24] P. A. Viola, Alignment by maximization of mutual information, Ph.D. thesis, Massachusetts Inst. Technol., Cambridge, 1995.

[25] L. Lemieux, U. C. Wieshmann, N. F. Moran, D. R. Fish, and S. D. Shoovon, "The detection and significance of subtle changes in mixed-signal brain lesions by serial MRI scan matching and spatial normalization", Med. Image Anal., Vol. 2, No. 3, pp. 227-242. 1998.

[26] F. Maes, A. Collignon, D. Vandermeulen, G. Marchal, and P. Suetens, "*Multimodality Image Registration by Maximization of Mutual Information*", IEEE Trans. Med. Imag., Vol. 16, No. 2, pp. 187-198, 1997.

[27] B. Kim, J. L. Boes, P. H. Bland, T. L. Chenevert, and C. R. Meyer, "*Motion Correction in fMRI via Registration of Individual Slices Into an Anatomical Volume*", Mag. Res. Med., Vol. 41, pp. 96-972, 1999.

[28] B. Kim, J. L. Boes, K. A. Frey, and C. R. Meyer, "*Mutual information for automated unwarping of rat brain autoradiography*", Neuroimage, Vol. 5, No. 1, pp. 31-40, 1997.

[29] C. Studholme, Measures of 3D medical image alignment, Ph.D. thesis, University of London, London, 1997.

[30] T. M. Buzug, J. Weese, C. Fassnacht, and C. Lorenz, "*Image Registration: Convex Weighting Functions for Histogram-Based Similarity Measures*", Lecture Notes in Computer Science, Berlin, Germany, Speringer-Verlag, pp. 203-212, 1997.

[31] M. Singh, L. Al-Dayeh, P. Patel, T.-S. Kim, C. Guclu, and O. Nalcioglu, "*Correction of Head Movements in Multi-Slice EPI and Single-Slice Gradient-Echo Functional MRI*", IEEE Trans. Nucl. Sci., Vol. 45, pp. 2162-2167, 1998.

[32] J. Weese, G. P. Penney, P. Desmedt, and T. M. Buzug, "*Pixel-Based 2D/3D Registration of Fluoroscopy Images and CT Scans for Image-Guided Surgery*", IEEE Trans. Inform. Technol. Biomed., Vol. 1, No. 4, pp. 284-293, 1997.

[33] L. Freire, A. Roche, and J.-F. Mangin, "*What is the Best Similarity Measure for Motion Correction in fMRI Time Series?*", IEEE Trans. Med. Imag., Vol. 21, No. 5, pp. 470-484, 2002.

[34] W. H. Press, S. A. Teukolsky, W. T. Vetterling, and B. P. Flannery, Numerical Recipes in C: The Art of Scientific Computing. Cambridge Press, Cambridge, 1992.

[35] G. K. Kanji, 100 Statistical Tests. SAGE Publications, Great Britain, 1993.

[36] R. A. Schowengerdt, Techniques for image processing and classification in remote sensing: Academic Press, New York, pp. 106-116, 1983.

[37] P. Cachier and X. Pennec, "2D Non-Rigid Registration by Gradient Descent on a Gaussin-Windowed Similarity Measure using Convolutions", IEEE Proc. Math. Methods in Biomed. Image Analysis, pp. 182-189, 2000.